sustainability

MDPI

Article

Carica papaya Crude Extracts Are an Efficient Source of Environmentally Friendly Biogenic Synthesizers of Silver Nanoparticles

Ghulam Zahara Jahangir [1,*], Tayyabah Anjum [1], Naim Rashid [2,*], Madeha Sadiq [1], Rida Farooq [1], Mubeen Akhtar [1], Sana Hussain [1], Anwaar Iftikhar [1], Muhammad Zafar Saleem [1] and Rehan Sadiq Shaikh [1]

[1] Centre for Applied Molecular Biology (CAMB), University of the Punjab, Lahore 54590, Pakistan
[2] Department of Water Resources Engineering & Management, National University of Science and Technology (NUST), Islamabad 44000, Pakistan
* Correspondence: zahra.camb@pu.edu.pk (G.Z.J.); naimkanwar@gmail.com (N.R.)

Abstract: Metallic nanoparticles are very useful, effective, and usually synthesized by toxic and expensive chemicals. Silver nanoparticles (AgNPs), measuring less than 100 nm, have shown promising impact in several biomedical investigations. These can inhibit microbial growth and aid in medicine administration. Six substrates of *Carica papaya* were used to synthesize silver nanoparticles that can limit the growth of bacteria and fungi. In this article, we report the synthesis of AgNPs from the leaf, seed, callus, peel, fruit juice, and bark of *Carica papaya*. AgNPs synthesized from callus showed the most promising results when tested against the growth of bacteria like *Xanthomonas campestris*, *Erwinia carotovera*, *Bacillus subtilis*, and fungi (*Aspergillus niger* and *Fusarium oxysporum*) when compared with other extracts' efficacy, and the callus was regenerated from petiole and midrib explants of *Carica papaya* in MS basal media supplemented with NAA and Kinetin (1 + 0.5 mg/L). A ratio of 1:20 of substrate extract to 1 mM $AgNO_3$ produced the most effective nanoparticles in terms of capping, quality, and stability when tested through surface plasmon resonance (SPR) within the 400–435 nm range. The nanoparticle sizes of all six types were measured using Image J software on micrographs of SEM at 200 nm resolution. The average diameters were analyzed through Origin software, and the finest AgNPs were observed to be synthesized from callus extract, i.e., 18.91 nm with rod-like morphology. Energy dispersive X-ray (EDX) at 2.6 keV revealed 43.38, 75.39, 70.611, 36.54, 58.57, and 45.94 percent elemental silver in AgNPs formed from the leaf, callus, juice, seed, bark, and peel extract, respectively. Silver nanoparticles synthesized from callus extract were smaller and exhibited the most effective antimicrobial potential, with the highest inhibitory zone of 19 mm against *Xanthomonas campestris* bacterium and up to 14 mm against *Aspergillus niger* fungus. Furthermore, the percentage of elemental Ag (measured through EDX) was found to be highest in the nanoparticles synthesized from callus compared to those synthesized from the leaf, seed, peel, fruit juice, and bark of *Carica papaya*. Hence, the callus extract is the most suitable substrate for the reduction of silver nitrate solution in 1:20 to form the finest silver nanoparticles in an effective biogenic way.

Keywords: papita; antidengue; nanobiotechnology; SEM; EDX; antibacterial; antifungal

check for updates

Citation: Jahangir, G.Z.; Anjum, T.; Rashid, N.; Sadiq, M.; Farooq, R.; Akhtar, M.; Hussain, S.; Iftikhar, A.; Saleem, M.Z.; Shaikh, R.S. *Carica papaya* Crude Extracts Are an Efficient Source of Environmentally Friendly Biogenic Synthesizers of Silver Nanoparticles. *Sustainability* **2023**, *15*, 16633. https://doi.org/10.3390/su152416633

Academic Editor: Marko Vinceković

Received: 29 August 2023
Revised: 7 October 2023
Accepted: 24 October 2023
Published: 7 December 2023

Copyright: © 2023 by the authors. Licensee MDPI, Basel, Switzerland. This article is an open access article distributed under the terms and conditions of the Creative Commons Attribution (CC BY) license (https://creativecommons.org/licenses/by/4.0/).

1. Introduction

The *Carica papaya*, often referred to as papita in Pakistan, is an angiosperm plant and belongs to the Caricaceae family. The *Carica papaya* is a perennial plant whose roots can be traced back to the southern part of Mexico [1]. *Carica papaya* is the third most extensively produced tropical fruit worldwide after mango and strawberry. Globally, it is cropped in about 60 countries, with a leading share from the Asian region, contributing almost 52.55 percent of the global bulk production of approximately 11.22 Mt [2]. *Carica papaya* holds immense potential for use in medicinal applications due to the presence of active phytochemicals. The leaf and seed extracts of *Carica papaya* have been shown to limit

microbial growth efficiently. It has been shown that flavonoid, one of the phytochemicals found in *Carica papaya* leaf extracts, inhibits the activity of proteases, an enzyme crucial to viral replication and assembly [3]. Because of the wide variety of biological benefits that can be accomplished with their incorporation, silver nanoparticles, commonly referred to as AgNPs, have emerged as the most significant category of metallic nanoparticles. Because of their extraordinarily small size, silver nanoparticles have shown tremendously beneficial effects in the biomedicine industry [4]. These silver nanoparticles have a large surface area compared to their total volume.

The application of nanomaterials has received immense popularity in nanomedicine and bio-nanotechnology. The biosynthesis of silver nanoparticles is possible through biological agents such as plant extracts, enzymes, fungi, etc., in addition to chemical procedures. Some compounds utilized in the chemical production of AgNPs, such as sodium borohydride, are toxic and can lead to various respiratory problems, including shortness of breath. So, the term "green nanotechnology" has become very popular quickly because it does not harm the environment and does not waste time or money [5]. The safe uses of silver nanoparticles (Ag-NPs) in various biological and biotechnological fields have garnered increased attention in recent decades. Antimicrobial, wound healing, antiviral, and anti-inflammatory applications, microbial control of phytopathogens, anticancer cell targeting, and optical receptors are just some of the recent uses for Ag-NPs. These have also been used as catalysts in chemistry, biosensors, antioxidants, and even for the delivery of DNA [6]. The novel stability, catalytic activity, biocompatibility, high conductivity, and huge surface area-to-volume ratio of Ag-NPs may account for their wide range of applications. Harnessing the metabolites of bacteria, fungi, yeast, algae, actinomycetes, and plants as reducing and capping agents can lead to a green synthesis of Ag-NPs in place of the harmful chemicals utilized in traditional chemical and physical production. The low cost, ease of use, scalability, eco-friendliness, and variety of metabolites produced by plants that facilitate plant-mediated green synthesis of Ag-NPs have all contributed to its increased popularity [7]. Furthermore, using nanoparticles in agriculture is attracting increased attention for plant protection and enhanced average yield. Fungi are eukaryotic microorganisms distinguished by their ability to invade and colonize plant tissues in various ways. Synthesized silver nanoparticles were tested for their antibacterial efficacy against a spectrum typically found in the laboratory [8].

Contamination due to general pathogenic bacterial and fungal strains is a significant problem for a laboratory involved in biotechnological protocols, especially animal and plant tissue culture. The presented study is a step towards developing cheaper nanomaterials to control laboratory contamination while working with biological experiments like cell culture and in vitro propagation of plants. The biosynthesis of silver nanoparticles was carried out using *Carica papaya* extracts because polyols act as an active functional group, causing silver nanoparticles to be capped earlier and reach stability more quickly. The preference of substrate (the papaya plant extracts) selection is based on its pharmacological properties and many medical applications. For forming AgNPs from the leaf, seed, callus, peel, fruit juice, and bark extracts of papaya, the reaction mixture ratio was optimized through spectrophotometry (surface plasmon resonance bands between 420 and 440 nm) using leaf extract as a reducing agent of $AgNO_3$. For molecular characterization of AgNPs, a scanning electron microscope (SEM) and an energy dispersive X-ray (EDX) were employed. Three strains of bacteria (*Xanthomonas campestris*, *Erwinia carotovera*, and *Bacillus subtilis*) were selected to evaluate antibacterial activity, and two strains of fungus (*Aspergillus niger* and *Fusarium oxysporum*) were selected to determine the antifungal activity of the produced silver nanoparticles using the leaf, seed, callus, peel, fruit juice, and bark extracts. The extract of bark (waste plant material) is a novel and previously unreported substrate in the biosynthesis of silver nanoparticles from *Carica papaya* plant extracts. Plant-mediated AgNPs have the potential for antimicrobial activity (antibacterial and antifungal), among the most important biological uses. For the first time, the effectiveness of silver nanoparticles synthesized from *Carica papaya* is being reported against the bacterial stem rot pathogen *Erwinia carotovera* and the black mold fungus *Aspergillus niger*.

2. Materials and Methods

Callus regeneration: The callus of *Carica papaya* was produced to obtain callus extract (used for silver nanoparticle synthesis). The potted plants of *Carica papaya* were purchased from the local market and planted in the field area of CAMB, Lahore, Pakistan. It was confirmed that the experimental samples, including the collection of materials, complied with relevant institutional, national, and international guidelines and legislation with appropriate permissions from authorities of the Centre for Applied Molecular Biology, University of the Punjab, Lahore, Pakistan. Midrib and petiole sections of young leaves were surface sterilized following the Malik et al. [9] method and inoculated in MS medium (Phytotech Labs, Lenexa, KS, USA) supplemented with 1.0 mg/L NAA and 0.5 mg/L. The callus cultures were generated and maintained at 23 ± 2 °C temperature, away from light.

The deposited material by Dr. Ghulum Zahara Jahangir (Assistant Professor, CAMB) is *Carica papaya* L., collected from a local commercial nursery (Faizan Nurzery, Model Town, Lahore, Pakistan). It has been allocated LAH20012 Herbarium, Institute of Botonym University of the Punjab, Lahore.

Preparation of extracts of *Carica papaya*: Various extracts were prepared following the methods reported for *Carica papaya* and other plants, like Komal and Arya [10] for leaf, Manisha et al. [11] for seed, Mude et al. [3] for callus, Pattanayak et al. [12] for bark, Jain et al. [13] for fruit juice, and Balavijayalakshmi and Ramalakshmi [14] for the extract from fruit peel. The extracts were stored at 4 °C until used.

Biogenesis and characterization of AgNPs: The reaction mixture (the quantities of plant extract and silver nitrate solution) was optimized following the basic methodology of Anjum et al. [15] with 1 mL of leaf extract and 1 mM of silver nitrate solution in 12 different ratios, i.e., *v*/*v* 1:1, 1:2, 1:3, 1:4, 1:5, 1:6, 1:7, 1:8, 1:9, 1:10, 1:15, and 1:20. The appropriate ratio of the reaction mixtures was selected based on the variation in color and intense absorption peak associated with surface plasmon resonance (SPR) bands. The spectral analysis of the reaction mixture was recorded in a UV-Vis spectrophotometer (BMS, UV2800) from 10 min to 120 min. AgNPs synthesized in a 420 mL reaction mixture from the respective extracts of leaf, callus, juice, seed, bark, and peel were centrifuged for 15 min, then 3 washings (of the pellet) with autoclaved distilled water followed by air-drying at room temperature and collection in 1.5 mL Eppendorf tubes were performed. Structural/morphological analysis was carried out through scanning electron microscopy (SEM; FEI Nova 450 Nano SEM) of dried pellet samples of AgNPs, and EDX was performed to determine the percentage of elemental silver by the commercial facility of the Department of Physics, Lahore University of Management Sciences (LUMS), Lahore, Pakistan. The scanning electron micrographs of AgNPs (synthesized from all extracts) captured at 200 nm resolution were inserted into Image J (ImageJ bundled with 64-bit Java8) for size estimation. The obtained data were analyzed through Origin software (Origin Viewer 2018) in histograms.

Antimicrobial activity of AgNPs: The antibacterial assay was performed on Gram (−) bacteria (*Xanthomonas campestris* and *Erwinia carotovera*) as well as Gram (+) bacteria (*Bacillus subtilis*) by the well diffusion method on Luria Bertani (LB) agar plates. A total of 100 µL of respective bacterial culture fresh grown to I.0 optical density in LB broth was spread and made into four wells with the back of a sterile micropipette tip (of 1000 µL) and placed on sterile filter paper disks in each well. In four different wells, 15 µL of the following were poured in each well: the sample (silver nanoparticles), 1 mM silver nitrate solution (SNS; positive control), 12.5 µg/mL tetracycline (antibiotic control), and the respective extract (negative control). The zone of inhibition was measured after overnight incubation at 37 °C. The effectivity of the same samples of AgNPs was also assessed against *Fusarium oxysporum* and *Aspergillus niger* fungi on potato dextrose agar plates by the earlier-described well diffusion method. A total of 50 µL of *Fusarium oxysporum* and *Aspergillus niger* spores were spread in the respective experiments. In four different wells, 25 µL of the following were poured, one in each well: the sample (silver nanoparticles), 1 mM SNS (positive control), 20 mg/L fluconazole (PFIZER, Diflucan 150 mg, antifungal

control), and the respective extract (negative control). The zone of inhibition was measured after 2 days of incubation at 37 °C.

Statistical Data Analysis: The data for antibacterial and antifungal assays were assessed statistically to determine the mean, variance, and significant difference. The data of the zone of inhibition (in mm) against bacterial and fungi strains are expressed as mean ± SD in the results.

3. Results

3.1. Callus Induction and Propagation

MS medium supplemented with NAA 1 mg/L and Kinetin 0.5 mg/L induced calluses in the petiole and midrib explants of *Carica papaya* within 4 weeks of incubation. The texture of the callus tissue formed from the petiole explant resembled cotton-like fibers during proliferation (Figure 1A), while the midrib explants produced nodular calluses (Figure 1B).

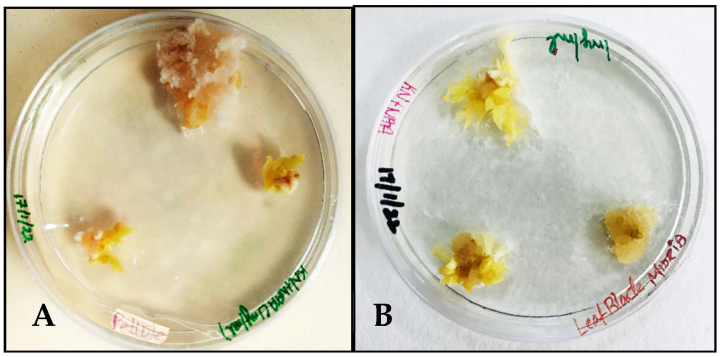


Figure 1. Callus induction in *Carica papaya's* MS + NAA 1 mg/L + Kinetin 0.5 mg/L: (**A**) from petiole explant; (**B**) from midrib explant.

3.2. Biosynthesis of AgNPs from Carica papaya Extracts

The reaction mixture was optimized with leaf extract (1 mL constant volume) and 12 different ratios of 1 mM SNS, i.e., *v*/*v* 1:1, 1:2, 1:3, 1:4, 1:5, 1:6, 1:7, 1:8, 1:9, 1:10, 1:15, and 1:20. A reddish-brown color developed quickly in 1:20 in comparison to other ratios; it suggested immediate and stable capping of AgNPs at that concentration (Figure 2). Spectrophotometric recordings in SPR bands revealed that absorbance in the 1:20 ratio at 425 nm was more stable than other tested ratios; even after one month, absorbance in the 1:20 ratio was stable (Figure 3). It reinforced the findings of the former experiment, i.e., a steady increase in stability and capping of AgNPs produced in leaf extract in the 1:20 ratio with 1 mM SNS. Afterward, AgNPs were successfully synthesized from the callus, juice, seed, bark, and peel extracts of *Carica papaya* in an established 1:20 ratio and obtained a reddish-brown color (Figure 4). Absorbance after 10, 20, 30, 60, 90, and 120 min revealed a steady increase in stability and capping of AgNPs. After incubation for 120 min, the SPR displayed clearly defined peaks and reached maximum stability (Figure 5).

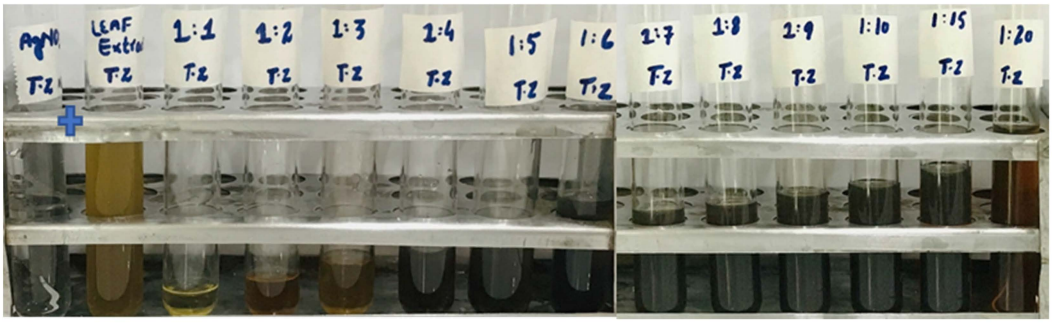


Figure 2. Biogenesis of AgNPs from *Carica papaya* leaf extract in water and 1 mM SNS in twelve ratios (1:1, 1:2, 1:3, 1:4, 1:5, 1:6, 1:7, 1:8, 1:9, 1:10, 1:15, 1:20); the reddish-brown color can be seen in the 1:20 ratio.

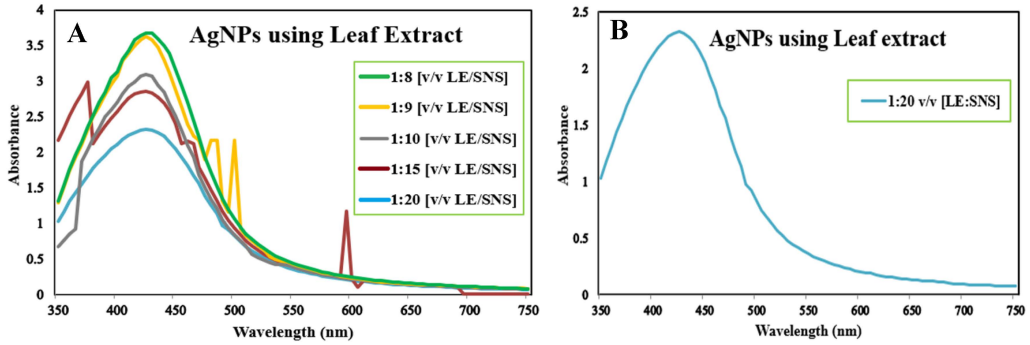


Figure 3. Surface plasmon resonance bands of reaction mixture containing *Carica papaya* leaf extract and 1 mM Silver nitrate solution in ratios 1:8, 1:9, 1:10, 1:15, 1:20 (**A**), and ratio 1:20 (**B**) at UV-Visible (BMS-UV2800).

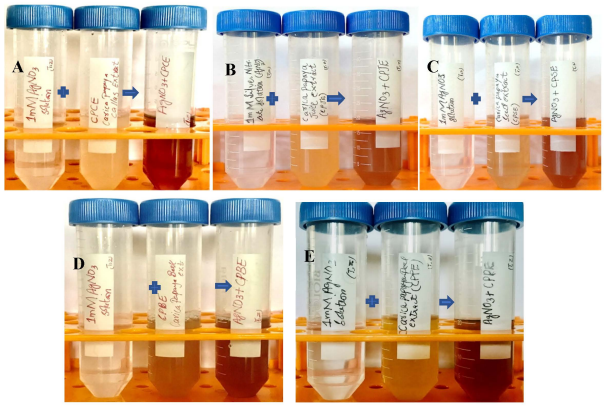


Figure 4. Biogenesis of AgNPs from *Carica papaya* extracts in water and 1 mM SNS in 1:20 ratio: the appearance of a reddish-brown color in callus extract (**A**); juice extract (**B**); seed extract (**C**); bark extract (**D**); and fruit peel extract (**E**) that indicates the synthesis of silver nanoparticles.

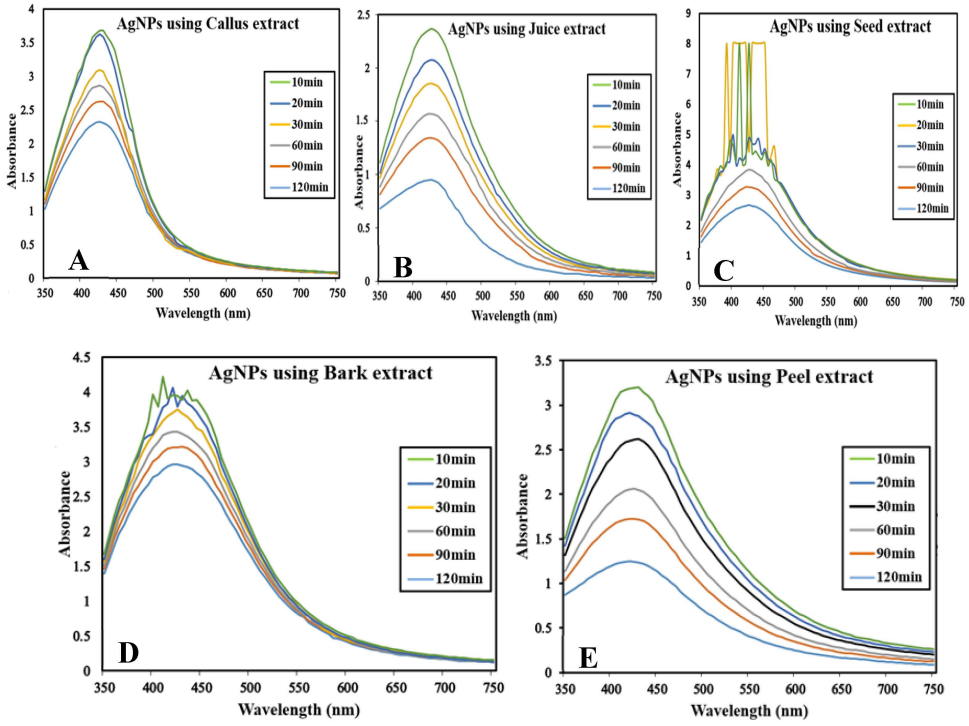


Figure 5. Surface plasmon resonance bands at different time intervals (at UV-Visible Spectrophotometer BMS-UV2800) containing reaction mixture in ratio 1:20 of *Carica papaya* extract and 1 mM Silver nitrate solution: (**A**) in callus extract; (**B**) in juice extract; (**C**) in seed extract; (**D**) in bark extract; and (**E**) in peel extract.

3.3. Characterization of AgNPs through SEM and XRD

The morphology of the AgNPs synthesized from various extracts of *Carica papaya* (leaf, callus, juice, seed, bark, and peel), studied at SEM, revealed nanorods, polydispersed, agglomerated, and triangular shapes. Size estimation (through Image J and Origin software) revealed the smallest size of AgNPs synthesized from the callus extract, i.e., 18.91 nm with rod-like morphology (Figure 6; Table 1). The bark, juice, seed, leaf, and peel extracts used as substrates for the synthesis of AgNPs resulted in particles with polydispersed and agglomerated morphologies with diameters of 32.69, 42.12, 65.83, 64.83, and 64.76 nm, respectively (Figure 6; Table 1). The comparison of scanning electron micrographs captured at a resolution of 10µm, 5µm, 2µm, 1µm, 500 nm, and 200 nm of AgNPs synthesized from different extracts like leaf extract, callus, juice, seed, bark, and peel (Figures 7–12, respectively) revealed that callus is the best substrate for biosynthesis using *Carica papaya.* The spectral data obtained from an energy dispersive X-ray (at 2.6 keV) has revealed defined peaks of pure Ag in all samples of nanoparticles synthesized from different extracts of *Carica papaya* (Figure 13). The highest concentration of elemental silver (75.39%) was calculated in AgNPs synthesized from the callus extract of *Carica papaya* (Figure 14). The Ag content of AgNPs synthesized from the leaf, juice, seed, bark, and peel extracts was recorded at 43.38%, 70.611%, 36.54%, 58.57%, and 45.94%, respectively (Figure 14).

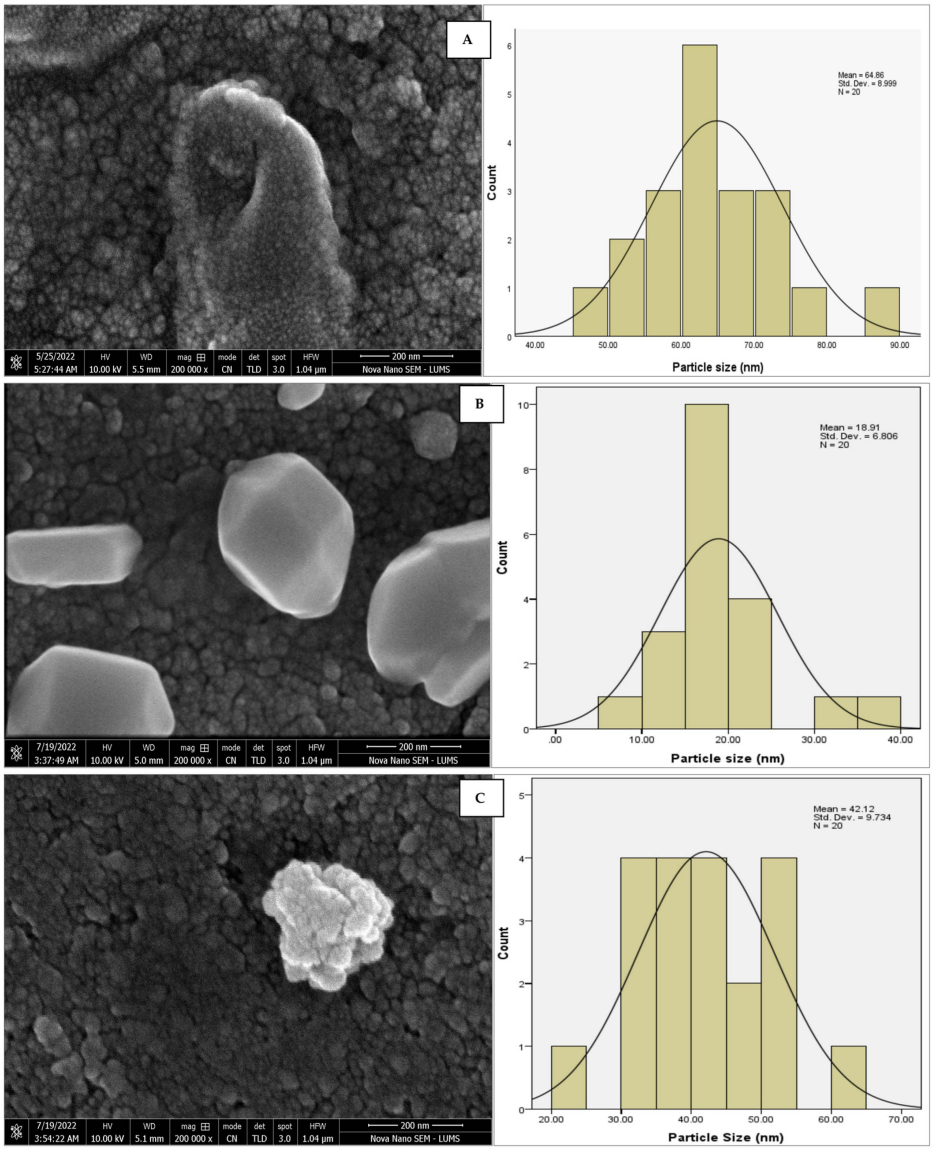


Figure 6. *Cont.*

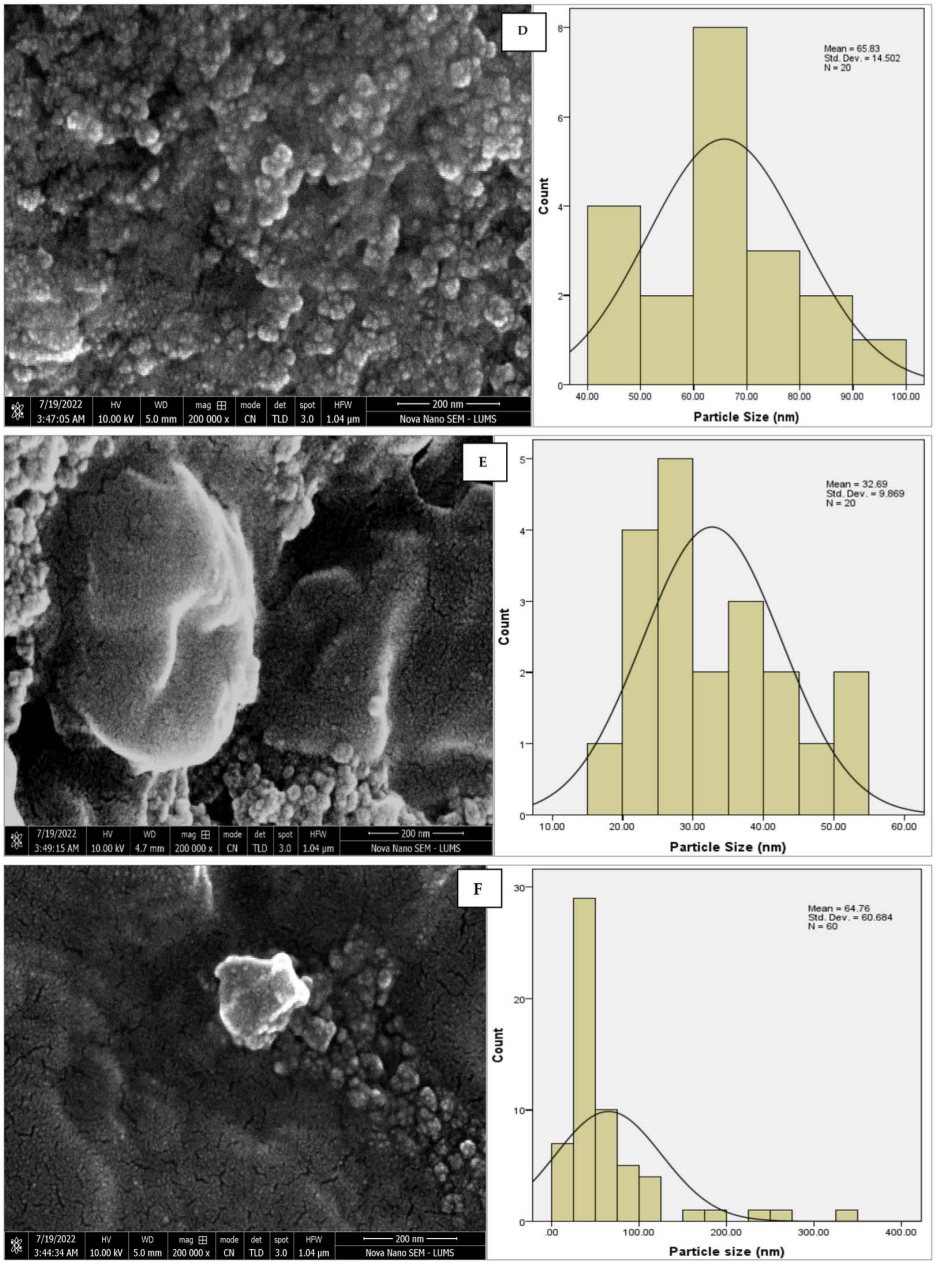


Figure 6. SEM micrographs with estimated histograms depicting average size distribution of AgNPs synthesized from (**A**) leaf extract 64.83 nm; (**B**) callus extract 18.91 nm; (**C**) juice extract 42.12 nm; (**D**) seed extract 65.83 nm; (**E**) bark extract 32.69 nm; and (**F**) peel extract 64.76 nm.

Table 1. Average diameters measured through and morphology of silver nanoparticles particles.

AgNPs Synthesized Using Plant Extract	Average Size Distribution (nm) of AgNPs	Shapes of AgNPs Observed in SEM
Leaf extract	64.83	Elongated rod type
Callus extract	18.91	Nano-rods and triangular
fruit Juice extract	42.12	Agglomerated
seed Extract	65.83	Polydispersed
bark Extract	32.69	Elongated rod type
peel Extract	64.76	Polydispersed

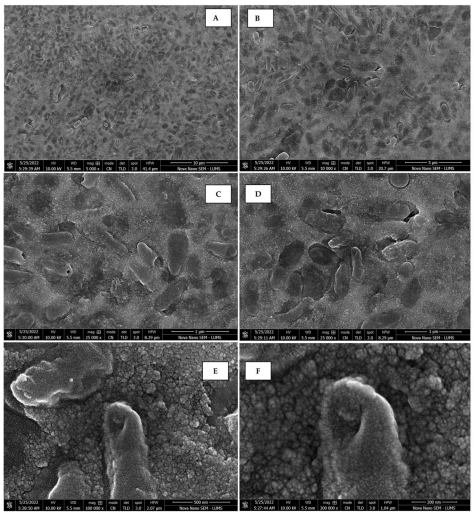


Figure 7. Scanning electron micrographs of AgNPs synthesized using leaf extract captured at resolutions of 10 µm (**A**); 5 µm (**B**); 2 µm (**C**); 1 µm (**D**); 500 nm (**E**); and 200 nm (**F**).

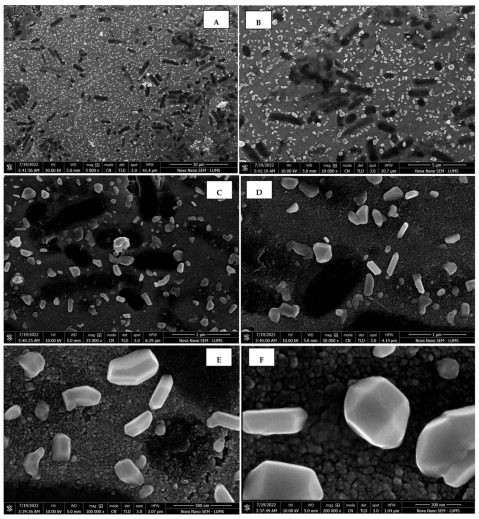


Figure 8. Scanning electron micrographs of AgNPs synthesized using callus extract captured at resolutions of 10 µm (**A**); 5 µm (**B**); 2 µm (**C**); 1 µm (**D**); 500 nm (**E**); and 200 nm (**F**).

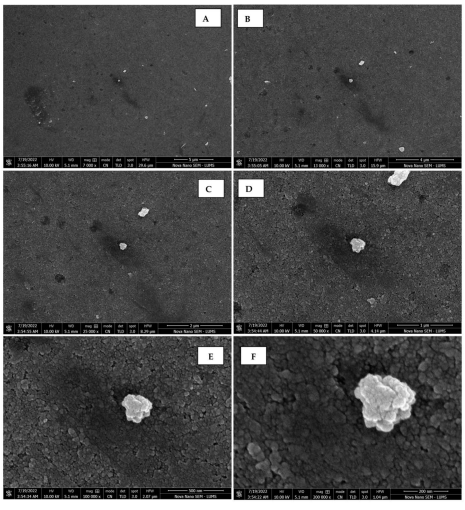


Figure 9. Scanning electron micrographs of AgNPs synthesized using fruit extract (juice) captured at resolutions of 10 µm (**A**); 5 µm (**B**); 2 µm (**C**); 1 µm (**D**); 500 nm (**E**); and 200 nm (**F**).

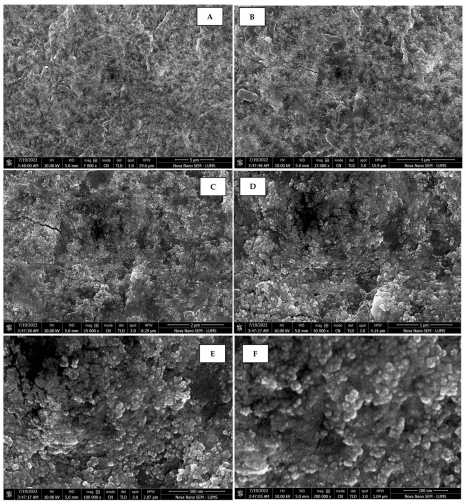


Figure 10. Scanning electron micrographs of AgNPs synthesized using seed extract captured at resolutions of 10 µm (**A**); 5 µm (**B**); 2 µm (**C**); 1 µm (**D**); 500 nm (**E**); and 200 nm (**F**).

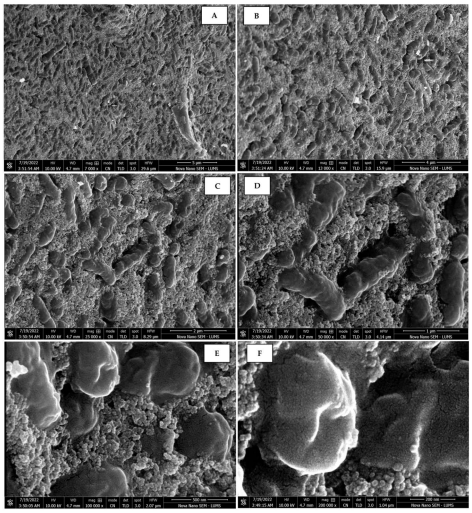


Figure 11. Scanning electron micrographs of AgNPs synthesized using bark extract captured at resolutions of 10 µm (**A**); 5 µm (**B**); 2 µm (**C**); 1 µm (**D**); 500 nm (**E**); and 200 nm (**F**).

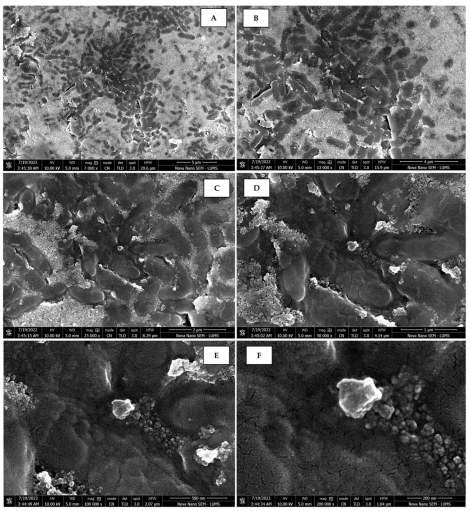


Figure 12. Scanning electron micrographs of AgNPs synthesized using peel extract captured at resolutions of 10 µm (**A**); 5 µm (**B**); 2 µm (**C**); 1 µm (**D**); 500 nm (**E**); and 200 nm (**F**).

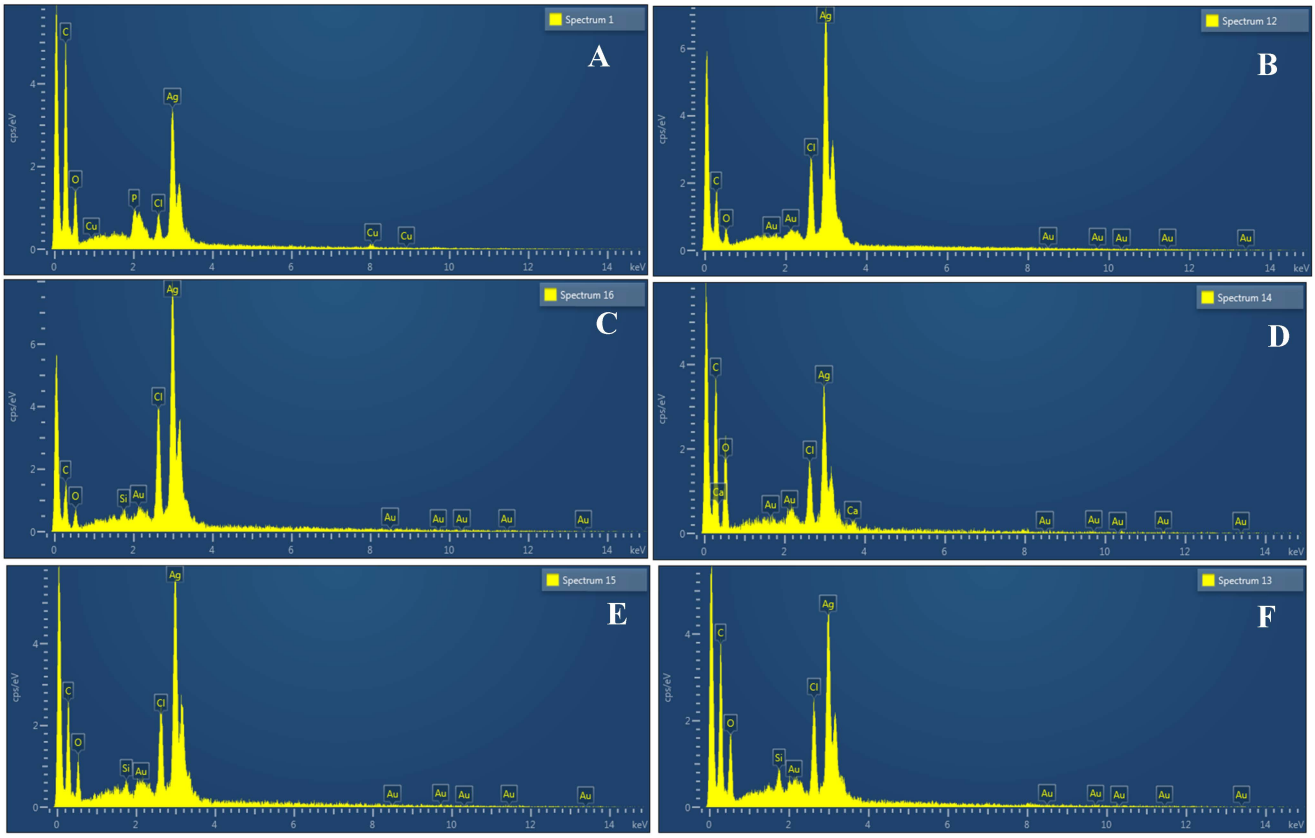


Figure 13. Spectra of EDX showing peaks of pure Ag in AgNPs samples synthesized using leaf extract (**A**); callus extract (**B**); juice extract (**C**); seed extract (**D**); bark extract (**E**); and peel extract (**F**).

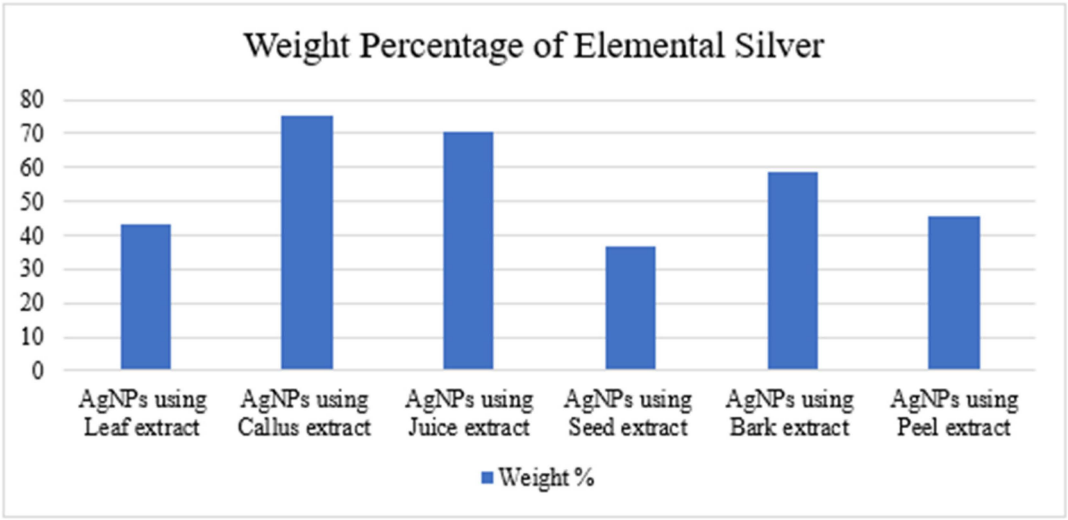


Figure 14. Weight percentage of pure elemental silver in AgNPs synthesized from leaf, callus, juice, seed, bark, and peel extracts.

3.4. Antimicrobial Activity

In determining the antibacterial effect of AgNPs produced from all six substrates of *Carica papaya*, the AgNPs exhibited strong efficacy to obstruct bacterial growth against *Xanthomonas campestris*, *Erwinia carotovera*, and *Bacillus subtilis* (Figures 15–17, respectively). After 24 h incubation, the measurements for the bactericidal zone of the respective AgNPs were wider than those of the standard antibacterial drug and also wider than those of their respective extracts (Figures 15–17). AgNPs formed from callus extract were most effective

against *Xanthomonas campestris*, with the highest inhibitory zone measuring 19 mm (Table 2, Figure 15). The AgNPs produced using peel extract were recorded to be the most efficient against *Erwinia carotovera,* with a 12 mm inhibitory zone (Table 2, Figure 16). The widest zone of inhibition against *Bacillus subtilis* was measured at 7.25 mm by AgNPs generated using seed extract (Table 2, Figure 17).

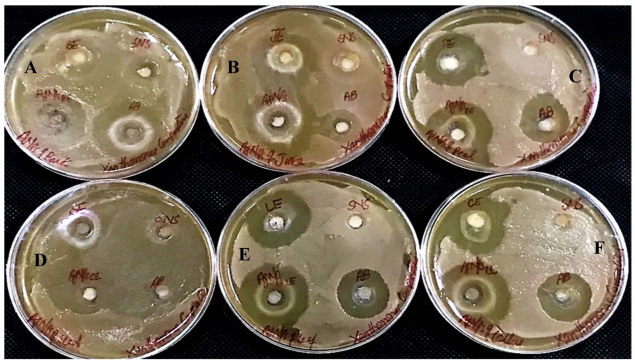


Figure 15. Antibacterial activity against *Xanthomonas campestris* has been shown by AgNPs synthesized using extracts of (**A**) bark; (**B**) juice; (**C**) peel; (**D**) seed; (**E**) leaves; and (**F**) callus.

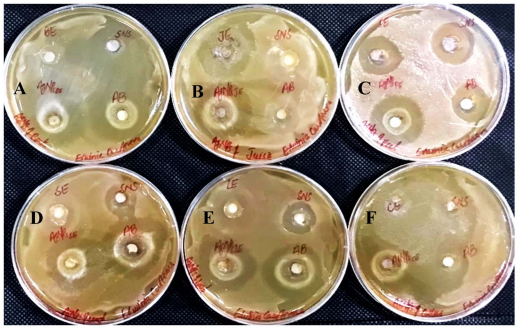


Figure 16. Antibacterial activity against *Erwinia Carotovera* has been shown by AgNPs synthesized using extracts of (**A**) bark; (**B**) juice; (**C**) peel; (**D**) seed; (**E**) leaves; and (**F**) callus.

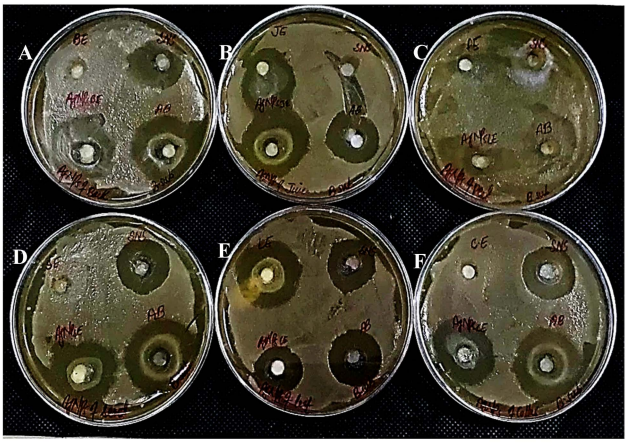


Figure 17. Antibacterial activity against *Bacillus subtilus* has been shown by AgNPs synthesized using extracts of (**A**) bark; (**B**) juice; (**C**) peel; (**D**) seed; (**E**) leaves; and (**F**) callus.

Table 2. Growth inhibition zone (in mm) caused by silver nanoparticles against *Bacillus subtilis*, *Erwinia Carotovera*, and *Xanthomonas Campestris* synthesized from six extracts of *Carica papaya*).

Bacterial Strain	Sample Type	Zone of Inhibition (mm) (15 µL/Well)					
		AgNPs of BE	AgNPs of JE	AgNPs of PE	AgNPs of SE	AgNPs of LE	AgNPs of CE
Xanthomonas campestris	Negative Control (extracts)	3 ± 0.96	5.5 ± 0.23	3 ± 1.54	6 ± 1.22	7.5 ± 1.2	8 ± 0.88
	Positive Control (SNS)	1.5 ± 0.41	1 ± 0.51	2 ± 0.77	2.5 ± 1.08	1.5 ± 0.15	1 ± 0.86
	AgNPs	12 ± 1.5	11 ± 1.74	17 ± 1.09	10 ± 2.13	18 ± 1.14	19 ± 1.42
	Tetracycline	14 ± 1.7	15 ± 2.64	10 ± 2.41	19 ± 2.93	20 ± 2.82	20 ± 2.92
Erwinia carotovera	Negative Control (extracts)	5 ± 0.7	5 ± 0.92	5 ± 0.9	5 ± 0.94	5.5 ± 1.19	6.5 ± 1.23
	Positive Control (SNS)	6 ± 1.07	7.5 ± 1.33	6.5 ± 1.1	8 ± 1.27	6.5 ± 1.4	7 ± 1.6
	AgNPs	7.5 ± 0.66	8.5 ± 1.64	12 ± 1.54	11 ± 1.25	10 ± 1.87	10 ± 1.15
	Tetracycline	10 ± 0.99	9.5 ± 1.79	11 ± 1.73	13 ± 1.55	14 ± 1.78	12 ± 1.23
Bacillus subtilis	Negative Control (extracts)	1 ± 0.31	6.5 ± 0.38	1.75 ± 1.0	1.5 ± 0.99	7 ± 1.2	1 ± 0.99
	Positive Control (SNS)	6.5 ± 0.64	4 ± 1.28	3.5 ± 1.20	5.5 ± 1.1	4 ± 1.56	4 ± 1.23
	AgNPs	6 ± 1.62	7 ± 1.55	6.5 ± 1.41	7.5 ± 1.3	7.25 ± 1.66	7 ± 1.62
	Tetracycline	7 ± 1.33	7 ± 1.42	4.5 ± 1.09	6 ± 1.2	7.5 ± 1.88	7.5 ± 1.52

The AgNPs synthesized from all six extracts of *Carica papaya* (juice, bark, callus, leaf, seed, and peel) significantly inhibited the growth of *Aspergillus niger* and *Fusarium oxysporum* fungi (Figures 18 and 19, respectively). AgNPs produced from callus extract most effectively inhibited the growth of *Aspergillus niger* (up to 14 mm). Other extracts also restricted growth at 13.5, 12.5, 10.5, and 8.5 mm by juice, bark, leaf, seed, and peel, respectively (Table 3, Figure 18). The growth of *Fusarium oxysporum* was effectively inhibited by AgNPs synthesized using fruit peel, seed, bark, and juice, but those that rose through the callus were most effective with a 7 mm zone of inhibition (Table 3, Figure 18).

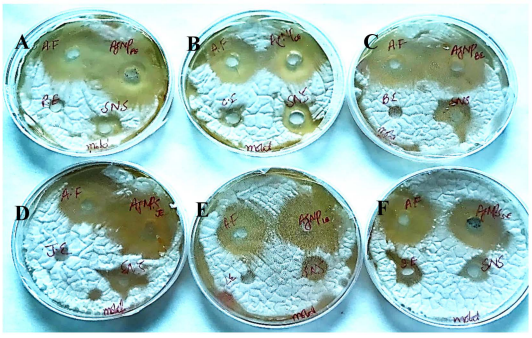


Figure 18. Antifungal activity of AgNPs synthesized using extracts of (**A**) peel; (**B**) callus; (**C**) bark; (**D**) juice; (**E**) leaf; and (**F**) seed against *Aspergillus niger*.

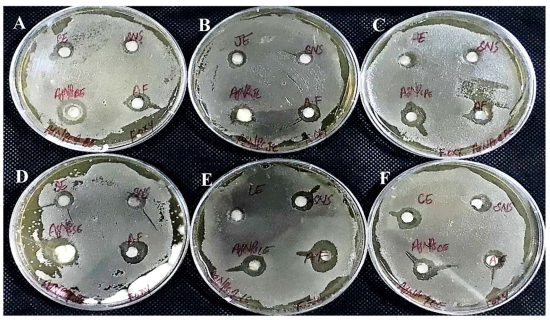


Figure 19. Antifungal activity of AgNPs synthesized using extracts of (**A**) bark; (**B**) fruit juice; (**C**) peel; (**D**) seed; (**E**) leaf; and (**F**) callus against *Fusarium oxysporum*.

Table 3. Growth of zone inhibition caused by silver nanoparticles against *Aspergillus niger* & *Fusarium oxysporum* synthesized from six extracts of *Carica papaya*).

Sample Type	Zone of Inhibition (mm) (15 µL/Well) against *Aspergillus niger*					
	AgNPs of PE	**AgNPs of CE**	**AgNPs of BE**	**AgNPs of JE**	**AgNPs of LE**	**AgNPs of SE**
Negative Control (Extract)	1 ± 0.99	2 ± 0.87	1 ± 0.65	1 ± 0.41	1 ± 0.88	2 ± 0.56
Positive Control (SNS)	5.0 ± 1.1	3.5 ± 1.56	4 ± 1.3	5 ± 1.5	3 ± 1.05	3 ± 1.08
AgNPs	14 ± 1.66	10 ± 1.98	12 ± 1.72	10 ± 1.71	12 ± 1.9	10 ± 1.23
Fluconazole	10 ± 1.67	9 ± 1.31	10 ± 1.98	9.75 ± 2.09	10 ± 1.74	11 ± 2.51
Sample Type	**Zone of Inhibition (mm) (15 µL/well) against *Fusarium oxysporum***					
	AgNPs of BE	**AgNPs of JE**	**AgNPs of PE**	**AgNPs of SE**	**AgNPs of LE**	**AgNPs of CE**
Negative Control (Extract)	3 ± 0.65	2 ± 0.23	1 ± 0.38	2 ± 1.07	1 ± 0.87	2 ± 1.1
Positive Control (SNS)	1 ± 0.45	1 ± 0.57	1 ± 0.99	1 ± 0.23	3 ± 1.1	2.5 ± 1.23
AgNPs	4 ± 1.56	3 ± 1.89	6 ± 1.27	4.5 ± 1.17	7 ± 2.1	4.5 ± 1.32
Fluconazole	6 ± 1.76	4 ± 1.13	8.5 ± 1.12	4.75 ± 1.56	8.5 ± 2.01	3.90 ± 2.45

4. Discussion

The callus cultures derived from medicinally important plants like *Carica papaya* have recently become an interesting prospect, and advancements in biotechnology have enabled their use as a successful tool for enhanced production of targeted phytochemicals like secondary metabolites from cell suspension cultures. Secondary metabolites are of interest because they can be produced easily and in enhanced quantities from plant cell cultures. Secondary metabolite concentrations, which are activated by elicitors and released as defense reactions, can be boosted by employing a cell suspension technique based on callus cultures [16]. Plant cells that can be cultured on a large scale to extract secondary metabolites could be grown using tissue culture techniques because they provide continuous, reliable, and renewable supplies of valuable plant medicines. Major benefits of cell culture systems over conventional cultivation include the elimination of environmental influences on plant growth (such as soil composition or climate) and the reduction in contamination sources and biotic and abiotic stresses that may affect plant growth in a natural system [16]. The callus induction and proliferation that have been recorded in this study are in close accordance with earlier published work. Malik et al. [9] reported the callus induction in *Carica papaya* from petiole and midrib explants in MS medium supplemented with NAA (1 mg/L), Kinetin (0.5 mg/L), and Cytokinins–Thidiazuron (TDZ). Despite the absence

of TDZ in the callusing medium, in the presented work, inoculated explants produced calluses. The callus cultures produced cottony fibers and callus textures similar to those reported by Malik et al. [9].

A 1:20 ratio was found to be more suitable for the synthesis of silver nanoparticles from the fresh leaf extract of the papaya plant. Hence, this ratio was practiced in all later experiments for the reduction of silver nitrate solution with various plant extracts' including bark, callus, leaf, seed, peel, and fruit juice. All extracts of the *Carica papaya* silver nitrate solution produced brown coloration in the 1:20 ratio, which was an indication that nanoparticles were produced. These findings are contradictory to those reported by Anjum et al. [15], who found the reddish-brown color in the 1:10 ratio among other reaction mixtures of plant extract and SNS for the biosynthesis of AgNPs using *Morus macroura*. The contradiction of findings may be due to variations in plant secondary products, as the source plant used for the preparation of plant extracts was different from that used in this study. Many other researchers have also reported successful production of silver nanoparticles from silvernitrate solution with reduction by fresh leaf extracts like *Camellia sinensis* [17] and *Murraya koenigii* plant [18]; however, this is the first report on the synthesis of AgNPs from waste material (the bark extract) of *Carica papaya,* and no published data are available.

For the confirmation of the synthesis and characterization of silver nanoparticles, the SPR bands (420–435 nm) were recorded in this report in experiments conducted with the callus, peel, bark, juice, seed, and bark extracts of *Carica papaya.* These findings are in close agreement with the work reported by Aina et al. [19], Balavijayalakshmi and Ramalakshmi [14], Mortazavi-Derazkola et al. [20], Pandit [21], and Zia and Chaudhary [22]. John et al. [23] comprehensively discussed the preparation of *Carica papaya* peel extract to synthesize the silver nanoparticles. They found the SPR band at 420–445 nm, a rod-like morphology, 70–95 nm-size particles, and the pure crystalline nature of silver through UV-Vis, SEM, TEM, and XRD, respectively [19]. The findings of Parsad et al. are different from the reported work as they have obtained UV-Vis Spectra at 402 nm in their report on the synthesis of AgNPs from leaf extracts of the *G. glauca* plant [24]. They have attributed the silver nanoparticle SPR excitation and their synthesis to maximum absorption at 402 nm. They have related the SPR to the abundance of free electrons on AgNPs and concluded that this linkage also influences the physical dimensions of AgNPs very significantly [24].

The morphological findings for the AgNPs that were obtained in this study are diverse for the AgNPs synthesized from various extracts of *Carica papaya,* like leaf, callus, juice, seed, bark, and peel. Nanorods, polydispersed, agglomerated, and triangular are the morphological shapes that were revealed during SEM. Similarly, the estimated size ranges were 32.69, 42.12, 65.83, 64.83, and 64.76 nm for the diameter of polydispersed and agglomerated morphologies in AgNPs synthesized from bark, juice, seed, leaf, and peel extracts, respectively. The smallest size was recorded for rod-like AgNPs synthesized from the callus extract of *Carica papaya,* i.e., 18.91 nm. The reported results of John et al. strengthen these findings, who found a rod-like morphology and a 70–95 nm size of the silver nanoparticles [23]. Other researchers like Anjum and Abbasi [25], Aref and Salem [26], and Mude et al. [3] reported the spherical and rod-like shapes of silver nanoparticles of 19, 17, and 30 nm sizes (respectively) synthesized with callus extract.

The antimicrobial potential of silver nanoparticles against three bacterial strains (*Xanthomonas campestris, Erwinia carotovera,* and *Bacillus subtilis*) and plant pathogenic fungal species (*Aspergillus niger* and *Fusarium oxysporum*) that are strong lab contaminants has been established in this report. The synthesized silver nanoparticles have been found to inhibit the growth of these strains successfully, even for many days. The antifungal and antibacterial potentials were higher than their respective aqueous extracts and even those of standard antifungal (Diflucan) and antibacterial (Tetracycline) positive controls. The precedent of earlier reports strengthens these findings, like those of Henry et al., who also found that aqueous extracts of *I. balsamina* and *L. camara* leaf were as effective against Gram-positive Staphylococcus aureus and Gram-negative *Escherichia coli* bacteria as a positive control, ciprofloxacin [27]. They further quoted that the same leaf extracts of *I. balsamina* and

L. camara containing Ag nanoparticles (3 mM and 5 mM Ag precursors) were more appropriate antibacterials and produced wider inhibition zones than those of ciprofloxacin [27]. Balavijayalakshmi and Ramalakshmi reported the effectiveness of the silver nanoparticles synthesized from Carica papaya peel against *Escherichia coli* and *Staphylococcus aureus* [14]. Mussin and Giusiano [28] further suggested that biogenic AgNPs perform much better as fungicidal agents when they are combined with antifungal drugs. Saxena and Ayushi [29] have reported the fungicidal characteristics of AgNPs synthesized even from the plant pathogenic fugal strain *S. sclerotiorum* MTCC 8785 against the *T. harzianum* strain. Findings of Zamana et al. [30] demonstrated that AgNPs were more effective antibacterials than conventional rifampicin as they obtained comparatively modest inhibition zones against gram-positive and gram-negative bacteria than those achieved by conventional rifampicin. Revathi et al. [31] and Arsene et al. [32] found that papaya's extracts are very effective reducing agents for the biogenic production of AgNPs; later, they further explained that AgNPs that are synthesized biologically using seed and root extract exhibit notable antibacterial as well as antibiofilm capabilities [32].

5. Conclusions

It was found that six water extracts of *Carica papaya* from the leaf, callus, seed, fruit juice, and waste material from the bark and fruit peel can be used to successfully synthesize AgNPs. The callus extract is very useful for the synthesis of high-quality silver nanoparticles. The surface plasmon resonance (SPR) band of each sample of synthesized AgNPs was determined within the range of 350 to 750 nm. AgNPs were successfully synthesized in extracts from the leaf, callus, seed, bark, juice, and peel, with the smallest size being found in the callus extract, containing the highest percentage of pure elemental silver of 75.39% and its nano-rod-shaped particles possessing a diameter of 18.9 nm, as confirmed by EDX and SEM, respectively. Silver nanoparticles synthesized from the leaves, calluses, juice, seeds, bark, and peels showed remarkable antibacterial and antifungal potential that was higher than their respective aqueous extracts and standard antifungal and antibacterial positive controls. Further, NAA and Kinetin (1 mg/L + 0.5 mg/L) proved the most suitable hormonal combination to be used in MS culture medium to generate bulk callus tissue from petiole and midrib explants.

Author Contributions: Conceptualization, G.Z.J., validation, G.Z.J. and N.R.; formal analysis, G.Z.J., N.R. and T.A.; investigation, G.Z.J., T.A., R.F., S.H., M.A., M.S. and A.I.; software, M.S.; resources, G.Z.J., M.Z.S. and R.S.S.; data curation, G.Z.J., N.R. and R.S.S.; writing—original draft preparation, G.Z.J. and T.A.; writing—review and editing, N.R. and M.Z.S.; supervision, G.Z.J. All authors have read and agreed to the published version of the manuscript.

Funding: This study received no external funding.

Institutional Review Board Statement: Not applicable.

Informed Consent Statement: Not applicable.

Data Availability Statement: All the data generated or analyzed are available in this article.

Acknowledgments: The authors are thankful to the University of the Punjab, Pakistan, for their scholastic support and grateful to all the cited authors for their useful data.

Conflicts of Interest: The authors declare no conflict of interest.

References

1. Lim, X.Y.; Chan, J.S.W.; Japri, N.; Lee, J.C.; Tan, T.Y.C. *Carica papaya* L. Leaf: A systematic scoping review on biological safety and herb-drug interactions. *Evid. Based Complement. Altern. Med.* **2021**, *7*, 5511221. [CrossRef]
2. FAOSTAT. *Crop Production*; FAO: Rome, Italy, 2012; Available online: http://faostat.fao.org/site/567/default.aspx#ancor (accessed on 19 September 2023).
3. Mude, N.; Ingle, A.; Gade, A.; Rai, M. Synthesis of silver nanoparticles using callus extract of *Carica papaya*—A first report. *J. Plant Biochem. Biotechnol.* **2009**, *18*, 83–86. [CrossRef]

4. Jimenez, B.C.; Johnson, M.E.; Bustos, A.R.M.; Murphy, K.E.; Winchester, M.R.; Baudrit, J.R.V. Silver nanoparticles: Technological advances, societal impacts, and metrological challenges. *Front. Chem.* **2017**, *39*, 113–123. [CrossRef]
5. Ahmad, S.; Munir, S.; Zeb, N.; Ullah, A.; Khan, B.; Ali, J.; Ali, S. Green nanotechnology: A review on green synthesis of silver nanoparticles—An ecofriendly approach. *Int. J. Nanomed.* **2019**, *14*, 5087–5107. [CrossRef]
6. Das, D.; Bhattacharyya, S.; Bhattacharyya, M.; Mandal, P. Green chemistry inspired formation of bioactive stable colloidal nanosilver and its wide-spectrum functionalised properties for sustainable industrial escalation. *Results Chem.* **2022**, *4*, 100533. [CrossRef]
7. Zofair, S.F.F.; Ahmad, S.; Hashmi, M.A.; Khan, S.H.; Khan, M.A.; Younus, H. Catalytic roles, immobilization and management of recalcitrant environmental pollutants by laccases: Significance in sustainable green chemistry. *J. Environ. Manag.* **2022**, *309*, 114676. [CrossRef]
8. Roy, T.S.; Fahim, M.R.; Islam, M.T.; Gafur, M.A.; Ferdous, T. Eco-friendly Synthesis of Silver Nanoparticles for Multifunctional Protective Cotton and Flax Fabrics. *J. Nat. Fibers* **2022**, *19*, 13681–13693. [CrossRef]
9. Malik, N.; Sengar, R.S.; Yadav, M.K.; Singh, S.K.; Singh, G.; Kumar, M. Effect of Different Plant Growth Regulators on In-Vitro Callus Induction in *Carica papaya*. *Int. J. Curr. Microbiol. Appl. Sci.* **2019**, *8*, 1217–1225. [CrossRef]
10. Komal, R.; Arya, V. Biosynthesis and characterization of silver nanoparticles from aqueous leaf extracts of *Carica papaya* and its antibacterial activity. *Int. J. Nanomater. Biostruct.* **2013**, *3*, 17–20.
11. Manisha, D.R.; Merugu, R.; Vijaybabu, A.R.; Pratap Rudra, M.P. Microwave-assisted biogenic synthesis of silver nanoparticles using dried seed extract of *Coriandrum sativum*, characterization and antimicrobial activity. *Int. J. ChemTech Res.* **2014**, *6*, 3957–3961.
12. Pattanayak, S.; Mollick, M.M.R.; Maity, D.; Chakraborty, S.; Dash, S.K.; Chattopadhyay, S.; Chakraborty, M. *Butea monosperma* bark extract mediated green synthesis of silver nanoparticles: Characterization and biomedical applications. *J. Saudi Chem. Soc.* **2017**, *21*, 673–684. [CrossRef]
13. Jain, D.; Daima, H.K.; Kachhwaha, S.; Kothari, S.L. Synthesis of plant-mediated silver nanoparticles using papaya fruit extract and evaluation of their antimicrobial activities. *Dig. J. Nanomater. Biostruct.* **2009**, *4*, 557–563.
14. Balavijayalakshmi, J.; Ramalakshmi, V. *Carica papaya* peel mediated synthesis of silver nanoparticles and its antibacterial activity against human pathogens. *J. Appl. Res. Technol.* **2017**, *15*, 413–422. [CrossRef]
15. Anjum, S.; Khan, A.K.; Qamar, A.; Fatima, N.; Drouet, S.; Renouard, S.; Hano, C. Light Tailoring: Impact of UV-C Irradiation on Biosynthesis, Physiognomies, and Clinical Activities of *Morus macroura*-Mediated Monometallic (Ag and ZnO) and Bimetallic (Ag–ZnO) Nanoparticles. *Int. J. Mol. Sci.* **2021**, *22*, 11294. [CrossRef] [PubMed]
16. Lashin, I.; Fouda, A.; Gobouri, A.A.; Azab, E.; Mohammedsaleh, Z.M.; Makharita, R.R. Antimicrobial and In Vitro Cytotoxic Efficacy of Biogenic Silver Nanoparticles (Ag-NPs) Fabricated by Callus Extract of *Solanum incanum* L. *Biomolecules* **2021**, *11*, 341. [CrossRef]
17. Göl, F.; Aygün, A.; Seyrankaya, A.; Gür, T.; Yenikaya, C.; Şen, F. Green synthesis and characterization of *Camellia sinensis* mediated silver nanoparticles for antibacterial ceramic applications. *Mater. Chem. Phys.* **2020**, *250*, 123037. [CrossRef]
18. Sarma, P.P.; Barman, K.; Baruah, P.K. Green synthesis of silver nanoparticles using *Murraya koenigii* leaf extract with efficient catalytic, antimicrobial, and sensing properties towards heavy metal ions. *Inorg. Chem. Commun.* **2023**, *152*, 110676. [CrossRef]
19. Aina, A.D.; Owolo, O.; Adeoye-Isijola, M.; Olukanni, O.D.; Lateef, A.; Egbe, T.; Abbas, S.H. Ecofriendly production of silver nanoparticles from the seeds of *Carica papaya* and its larvicidal and antibacterial efficacy against some selected bacterial pathogens. *IOP Conf. Ser. Mater. Sci. Eng.* **2020**, *805*, 12–38. [CrossRef]
20. Mortazavi-Derazkola, S.; Yousefinia, A.; Naghizadeh, A.; Lashkari, S.; Hosseinzadeh, M. Green synthesis and characterization of silver nanoparticles using *Elaeagnus angustifolia* bark extract and study of Its antibacterial effect. *J. Polym. Environ.* **2021**, *29*, 3539–3547. [CrossRef]
21. Pandit, R. Green synthesis of silver nanoparticles from seed extract of *Brassica nigra* and its antibacterial activity. *Nusant. Biosci.* **2015**, *7*, 15–19. [CrossRef]
22. Zia, M.; Chaudhary, M.F. Green synthesis of silver nanoparticles from grape and tomato juices and evaluation of biological activities. *IET Nanobiotechnol.* **2017**, *11*, 193–199. [CrossRef] [PubMed]
23. John, T.; Parmar, K.A.; Kotval, S.C.; Jadhav, J. Synthesis, characterization, antibacterial and anticancer properties of silver nanoparticles synthesized from *Carica papaya* peel extract. *Int. J. Nanosci. Nanotechnol.* **2021**, *17*, 23–32.
24. Prasad, S.R.; Teli, S.B.; Ghosh, J.; Prasad, N.R.; Shaikh, V.S.; Nazeruddin, G.M.; Al-Sehemi, A.G.; Patel, I.; Shaikh, Y.I. A review on bio-inspired synthesis of silver nanoparticles: Their antimicrobial efficacy and toxicity. *Eng. Sci.* **2021**, *16*, 90–128. [CrossRef]
25. Anjum, S.; Abbasi, B.H. Thidiazuron-enhanced biosynthesis and antimicrobial efficacy of silver nanoparticles via improving phytochemical reducing potential in callus culture of *Linum usitatissimum* L. *Int. J. Nanomed.* **2016**, *11*, 715–728. [CrossRef]
26. Aref, M.S.; Salem, S.S. Bio-callus synthesis of silver nanoparticles, characterization, and antibacterial activities via *Cinnamomum camphora* callus culture. *Biocatal. Agric. Biotechnol.* **2020**, *27*, 77–90. [CrossRef]
27. Aritonang, H.F.; Koleangan, H.; Wuntu, A.D. Synthesis of Silver Nanoparticles Using Aqueous Extract of Medicinal Plants' (*Impatiens balsamina* and *Lantana camara*) Fresh Leaves and Analysis of Antimicrobial Activity. *Int. J. Microbiol.* **2019**, *2019*, 8642303. [CrossRef]
28. Mussin, J.; Giusiano, G. Biogenic silver nanoparticles as antifungal agents. *Front. Chem.* **2022**, *10*, 1023542. [CrossRef] [PubMed]

29. Saxena, J.; Ayushi, K.M. Evaluation of *Sclerotinia sclerotiorum* MTCC 8785 as a biological agent for the synthesis of silver nanoparticles and assessment of their antifungal potential against *Trichoderma harzianum* MTCC 801. *Environ. Res.* **2023**, *216*, 114752. [CrossRef]
30. Zamana, Y.; Ishaquea, M.Z.; Sattarb, R.; Rehmanb, M.M.; Sabac, I.; Kanwala, S.; Akrama, M.; Shahzada, M.; Kanwald, H.; Qadirb, R.; et al. Antibacterial potential of silver nanoparticles synthesized using tri-sodium citrate via controlled exploitation of temperature. *Dig. J. Nanomater. Biostruct.* **2022**, *17*, 979–987. [CrossRef]
31. Revathi, E.; Yaku, G.; Unnisa, S.A.; Malyala, P.; Praveen, V. Microwave assisted green synthesis of silver nanoparticles from Carica papaya fruit extract: Characterization and detection of Fe3+ and Hg2+ ions. *Mater. Today Proc.* **2023**. [CrossRef]
32. Arsene, M.M.J.; Viktorovna, P.I.; Alla, M.; Mariya, M.; Davares, A.K.L.; Carime, B.Z.; Anatolievna, G.O.; Vyacheslavovna, Y.N.; Vladimirovna, Z.A.; Andreevna, S.L.; et al. Antimicrobial activity of phytofabricated silver nanoparticles using *Carica papaya* L. against Gram-negative bacteria. *Vet. World* **2023**, *16*, 1301. [CrossRef] [PubMed]

Disclaimer/Publisher's Note: The statements, opinions and data contained in all publications are solely those of the individual author(s) and contributor(s) and not of MDPI and/or the editor(s). MDPI and/or the editor(s) disclaim responsibility for any injury to people or property resulting from any ideas, methods, instructions or products referred to in the content.